Organic Nanostructures

Edited by
Jerry L. Atwood and Jonathan W. Steed

WILEY-VCH Verlag GmbH & Co. KGaA

Organic Nanostructures

Edited by
Jerry L. Atwood and Jonathan W. Steed

Related Titles

Vollath, D.

Nanomaterials

An Introduction to Synthesis, Characterization and Processing

approx. 200 pages with approx. 220 figures and approx. 20 tables
Softcover
ISBN: 978-3-527-31531-4

Zehetbauer, M. J., Zhu, Y. T. (eds.)

Bulk Nanostructured Materials

approx. 750 pages with approx. 250 figures and approx. 20 tables
2008
Hardcover
ISBN: 978-3-527-31524-6

Astruc, D. (ed.)

Nanoparticles and Catalysis

approx. 672 pages in 2 volumes with approx. 850 figures
2007
Hardcover
ISBN: 978-3-527-31572-7

Rao, C. N. R., Müller, A., Cheetham, A. K. (eds.)

Nanomaterials Chemistry

Recent Developments and New Directions

420 pages with 190 figures and 9 tables
2007
Hardcover
ISBN: 978-3-527-31664-9

Organic Nanostructures

Edited by
Jerry L. Atwood and Jonathan W. Steed

WILEY-VCH Verlag GmbH & Co. KGaA

The Editors

Prof. Dr. Jerry L. Atwood
University of Missouri–Columbia
Department of Chemistry
125 Chemistry Building
Columbia, MO 65211
USA

Prof. Jonathan W. Steed
University of Durham
Department of Chemistry
South Road
Durham, DH1 3LE
United Kingdom

Cover illustration
The front cover shows a space-filling image illustrating the packing of the ligands in the optically pure cage complex $[Zn_4(L^{o\text{-}Ph*})_6(ClO_4)](ClO_4)_7$ and is adapted from Figure 9.5 with the permission of Michael Ward. The structure is superimposed on an SEM image of the helical fibrous structure of a chiral supramolecular xerogel.

Library of Congress Card No.: applied for

British Library Cataloguing-in-Publication Data
A catalogue record for this book is available from the British Library.

Bibliographic information published by the Deutsche Nationalbibliothek
Die Deutsche Nationalbibliothek lists this publication in the Deutsche Nationalbibliografie; detailed bibliographic data are available in the Internet at <http://dnb.d-nb.de>.

Typesetting Thomson Digital, Noida, India
Printing Strauss GmbH, Mörlenbach
Binding Litges & Dopf GmbH, Heppenheim

Printed in the Federal Republic of Germany
Printed on acid-free paper

ISBN: 978-3-527-31836-0

In memory of Professor Dimitry M. Rudkevich
(1963–2007)

Contents

Preface

Current research in chemistry and materials science is now vigorously pushing the boundaries of the components studied firmly into the multi-nanometer length scale. In terms of traditional "molecules" a nanometer (10^{-9} m) is relatively large. As a result, it is only relatively recent advances in analytical instrumentation capable of delivering a molecular-level understanding of structure and properties in this kind of size regime that have allowed access to and the study of such large molecules and assemblies. The key interest in multi-nanometer-scale structures (nanostructures) is the fact that their size allows them to exhibit a significant degree of functionality and complexity – complexity that is mirrored in biological systems such as enzymes and polynucleotides, Nature's own nanostructures. However, this functionality is compressed into a space that is very small on the human scale, sparking interest in fields such as molecular computing and molecular devices. Thus one of the great opening frontiers in molecular sciences is the upward synthesis, understanding of structure and application of molecules and molecular concepts into the nanoscale.

In compiling this book we have sought to bring together chapters from leading experts working on the cutting edge of this revolution on the nanoscale. Each chapter is a self-contained illustration of the way in which the nanoscale view is influencing current thinking and research across the molecular sciences. The focus is on the "organic" (loosely applied) since it is generally carbon-based building blocks that are the most versatile molecular components that can be induced to link into nanoscale structures. As chapters by Mohammed Eddaoudi and Lee Cronin show, however, hybrid organic–inorganic materials and well-defined inorganic building blocks as just as capable of assembling into well-defined and well-characterized discrete and polymeric nanostructures.

Crucial to the whole field of nanochemistry is the cross-fertilization between researchers from different disciplines that are approaching related structures from very different perspectives. It is with this aspect in mind that we have deliberately mixed together contributions from the solid-state materials community as in Dario Braga's perspective on the crystal engineering or organic nanostructures and from experts in discrete molecular assemblies such as Dimitry Rudkevich, Kay Severin, Thomas Rauchfuss and Bruce Gibb. Of course, nanostructures are not

always so well defined and so these aspects are balanced nicely by David Smith's chapter on gel-phase materials – in some respects a "halfway house" between solution-phase and solid-state assemblies. We also felt it of key importance to illustrate ways to use small-scale molecular concepts in order to "synthesize-up" nanostructures. Chapters by Paul Beer, Steve Loeb and Len MacGillivray provide very different perspectives on templation and assembly in the field, while Makoto Fujita and Mike Ward deal with larger-scale self-assembly. Finally, all-important functional nanostructured devices are illustrated by Vincenzo Balzani's chapter.

Although a book of this size can only be illustrative of such a burgeoning field, it is our sincere hope that the juxtaposition of these different perspectives and systems in one place will stimulate and contribute to the ongoing process of cross-fertilization that is driving this fascinating and emerging area of molecular science. It has certainly been a fascinating and pleasurable experience to work on this project and we thank all of the authors wholeheartedly for their enthusiastic contributions to this project. We are grateful also to Manfred Köhl and Steffen Pauly at Wiley-VCH for their belief in the book and for their help in making it a reality. As this book went to press we learned of the sad and untimely death of Dimitry Rudkevich. We would like to dedicate this book to his memory and legacy to science.

December 2007

Jonathan W. Steed, Durham, UK
Jerry L. Atwood, Columbia, MO, USA

List of Contributors

Jerry L. Atwood
University of Missouri–Columbia
Department of Chemistry
125 Chemistry Building
MO 65211 Columbia
USA

Vincenzo Balzani
Università di Bologna
Dipartimento di Chimica "G. Ciamician"
Via Selmi 2
40126 Bologna
Italy

Paul D. Beer
University of Oxford
Department of Chemistry
Inorganic Chemistry Laboratory
South Parks Road
Oxford OX1 3QR
UK

Dario Braga
Università di Bologna
Dipartimento di Chimica "G. Ciamician"
Via Selmi 2
40126 Bologna
Italy

Dejan-Krešimir Bučar
University of Iowa
Department of Chemistry
Iowa City
IA 52245
USA

Michał J. Chmielewski
University of Oxford
Department of Chemistry
Inorganic Chemistry Laboratory
South Parks Road
Oxford OX1 3QR
UK

Alberto Credi
Università di Bologna
Dipartimento di Chimica "G. Ciamician"
Via Selmi 2
40126 Bologna
Italy

Leroy Cronin
University of Glasgow
Department of Chemistry
Glasgow G12 8QQ
UK

Marco Curzi
Università di Bologna
Dipartimento di Chimica "G. Ciamician"
Via Selmi 2
40126 Bologna
Italy

Scott J. Dalgarno
Heriot–Watt University
School of Engineering and Physical Sciences – Chemistry
Edinburgh EH14 4AS
UK

Mohamed Eddaoudi
University of South Florida
Department of Chemistry
4202 East Fowler Avenue (CHE 205)
Tampa
FL 33620
USA

Jarrod F. Eubank
University of South Florida
Department of Chemistry
4202 East Fowler Avenue (CHE 205)
Tampa
FL 33620
USA

Makoto Fujita
The University of Tokyo
School of Engineering
Department of Applied Chemistry
7-3-1 Hongo
Bunkyo-ku
Tokyo 113-8656
Japan

Stefano Luca Giaffreda
Università di Bologna
Dipartimento di Chimica "G. Ciamician"
Via Selmi 2
40126 Bologna
Italy

Bruce C. Gibb
University of New Orleans
Department of Chemistry
New Orleans
LA 70148
USA

Fabrizia Grepioni
Università di Bologna
Dipartimento di Chimica "G. Ciamician"
Via Selmi 2
40126 Bologna
Italy

Tamara D. Hamilton
University of Iowa
Department of Chemistry
Iowa City
IA 52245
USA

Stephen J. Loeb
University of Windsor
Department of Chemistry and Biochemistry
Windsor
Ontario N9B 3P4
Canada

Leonard R. MacGillivray
University of Iowa
Department of Chemistry
Iowa City
IA 52245
USA

Lucia Maini
Università di Bologna
Dipartimento di Chimica "G. Ciamician"
Via Selmi 2
40126 Bologna
Italy

Charalampos Moiras
University of Glasgow
Department of Chemistry
Glasgow G12 8QQ
UK

Takashi Murase
The University of Tokyo
School of Engineering
Department of Applied Chemistry
7-3-1 Hongo
Bunkyo-ku
Tokyo 113-8656
Japan

Voltaire G. Organo
University of Texas at Arlington
Department of Chemistry and
Biochemistry
Arlington
TX 76019-0065
USA

Anna Pettersen
Università di Bologna
Dipartimento di Chimica "G. Ciamician"
Via Selmi 2
40126 Bologna
Italy

Marco Polito
Università di Bologna
Dipartimento di Chimica "G. Ciamician"
Via Selmi 2
40126 Bologna
Italy

Nicholas P. Power
University of Missouri–Columbia
Department of Chemistry
125 Chemistry Building
MO 65211 Columbia
USA

Thomas B. Rauchfuss
University of Illinois
Department of Chemistry
Urbana
IL 61801
USA

Dmitry M. Rudkevich
University of Texas at Arlington
Department of Chemistry and
Biochemistry
Arlington
TX 76019-0065
USA

Kay Severin
École Polytechnique Fédérale de
Lausanne
Institut des Sciences et Ingénierie
Chimiques
CH-1015 Lausanne
Switzerland

David K. Smith
University of York
Department of Chemistry
Heslington
York YO10 5DD
UK

Margherita Venturi
Università di Bologna
Dipartimento di Chimica "G. Ciamician"
Via Selmi 2
40126 Bologna
Italy

Michael D. Ward
University of Sheffield
Department of Chemistry
Dainton Building
Sheffield S3 7HF
UK

1
Artificial Photochemical Devices and Machines

Vincenzo Balzani, Alberto Credi, and Margherita Venturi

1.1
Introduction

The interaction between light and matter lies at the heart of the most important processes of life [1]. Photons are exploited by natural systems as both quanta of energy and elements of information. Light constitutes an energy source and is consumed (or, more precisely, converted) in large amount in the natural photosynthetic process, whereas it plays the role of a signal in vision-related processes, where the energy used to run the operation is biological in nature.

A variety of functions can also be obtained from the interaction between light and matter in artificial systems [2]. The type and utility of such functions depend on the degree of complexity and organization of the chemical systems that receive and process the photons.

About 20 years ago, in the frame of research on supramolecular chemistry, the idea began to arise [3–5] that the concept of macroscopic device and machine can be transferred to the molecular level. In short, a molecular device can be defined [6] as an assembly of a discrete number of molecular components designed to perform a function under appropriate external stimulation. A molecular machine [6–8] is a particular type of device where the function is achieved through the mechanical movements of its molecular components.

In analogy with their macroscopic counterparts, molecular devices and machines need energy to operate and signal to communicate with the operator. Light provides an answer to this dual requirement. Indeed, a great number of molecular devices and machines are powered by light-induced processes and light can also be useful to "read" the state of the system and thus to control and monitor its operation. Before illustrating examples of artificial photochemical molecular devices and machines, it is worthwhile recalling a few basic aspects of the interaction between molecular and supramolecular systems and light. For a more detailed discussion, books [9–15] can be consulted.

1.2
Molecular and Supramolecular Photochemistry

1.2.1
Molecular Photochemistry

Figure 1.1 shows a schematic energy level diagram for a generic molecule that could also be a component of a supramolecular species. In most cases the ground state of a molecule is a singlet state (S_0) and the excited states are either singlets (S_1, S_2, etc.) or triplets (T_1, T_2, etc.). In principle, transitions between states having the same spin value are allowed, whereas those between states of different spin are forbidden. Therefore, the electronic absorption bands observed in the UV–visible spectrum of molecules usually correspond to $S_0 \rightarrow S_n$ transitions. The excited states so obtained are unstable species that decay by rapid first-order kinetic processes, namely chemical reactions (e.g. dissociation, isomerization) and/or radiative and nonradiative deactivations. In the discussion that follows, excited-state reactions do not need to be explicitly considered and can formally be incorporated within the radiationless decay processes. When a molecule is excited to upper singlet excited states (Figure 1.1), it usually undergoes a rapid and 100% efficient radiationless deactivation [internal conversion (ic)] to the lowest excited singlet, S_1. Such an excited state undergoes deactivation via three competing processes: nonradiative decay to the ground state (internal conversion, rate constant k_{ic}); radiative decay to the ground state (fluorescence, k_{fl}); conversion to the lowest triplet state T_1 (intersystem crossing, k_{isc}). In its turn, T_1 can undergo deactivation via nonradiative (intersystem crossing, k'_{isc}) or radiative (phosphorescence, k_{ph}) decay to the ground state S_0. When the molecule contains heavy atoms, the formally forbidden intersystem crossing and

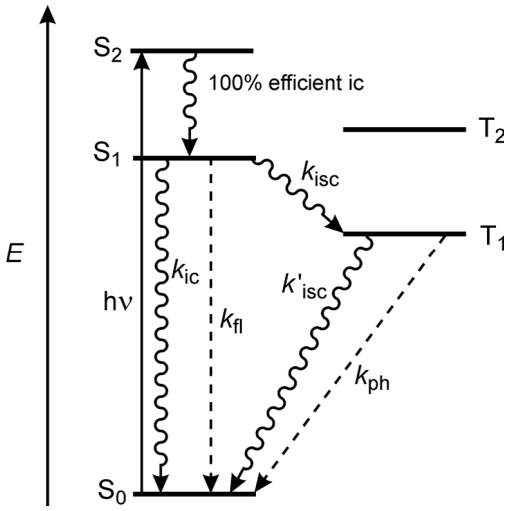

Figure 1.1 Schematic energy level diagram for a generic molecule. For more details, see text.

phosphorescence processes become faster. The lifetime (τ) of an excited state, that is, the time needed to reduce the excited-state concentration by 2.718 (i.e. the basis for natural logarithms, e), is given by the reciprocal of the summation of the deactivation rate constants:

$$\tau(S_1) = \frac{1}{(k_{ic}+k_{fl}+k_{isc})} \tag{1}$$

$$\tau(T_1) = \frac{1}{(k'_{isc}+k_{ph})} \tag{2}$$

The orders of magnitude of $\tau(S_1)$ and $\tau(T_1)$ are approximately $10^{-9}-10^{-7}$ and $10^{-3}-10^{0}$ s, respectively. The quantum yield of fluorescence (ratio between the number of photons emitted by S_1 and the number of absorbed photons) and phosphorescence (ratio between the number of photons emitted by T_1 and the number of absorbed photons) can range between 0 and 1 and are given by

$$\Phi_{fl} = \frac{k_{fl}}{(k_{ic}+k_{fl}+k_{isc})} \tag{3}$$

$$\Phi_{ph} = \frac{k_{ph} \times k_{isc}}{(k'_{isc}+k_{ph}) \times (k_{ic}+k_{fl}+k_{isc})} \tag{4}$$

Excited-state lifetimes and fluorescence and phosphorescence quantum yields of a great number of molecules are known [16].

When the intramolecular deactivation processes are not too fast, that is, when the lifetime of the excited state is sufficiently long, an excited molecule $^*A$ may have a chance to encounter a molecule of another solute, B (Figure 1.2). In such a case, some specific interaction can occur leading to the deactivation of the excited state by second-order kinetic processes. The two most important types of interactions in an encounter are those leading to electron or energy transfer. The occurrence of these processes causes the quenching of the intrinsic properties of $^*A$; energy transfer also

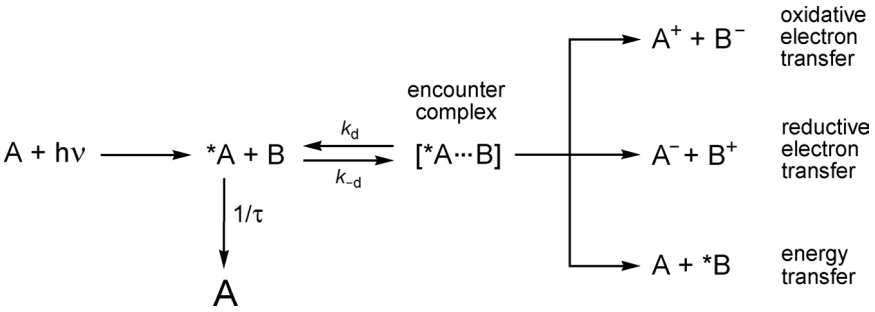

Figure 1.2 Schematic representation of bimolecular electron- and energy-transfer processes that may occur following an encounter between an excited state, $^*A$, and another chemical species, B.

leads to sensitization of the excited-state properties of the B species. Simple kinetic arguments show that only the excited states that live longer than ca. 10^{-9} s may have a chance to be involved in encounters with other solute molecules.

An electronically excited state is a species with completely different properties to those of the ground-state molecule. In particular, because of its higher energy content, an excited state is both a stronger reductant and a stronger oxidant than the corresponding ground state [17]. To a first approximation, the redox potential of an excited-state couple may be calculated from the potential of the related ground-state couple and the one-electron potential corresponding to the zero–zero excited-state energy, $E^{0\text{–}0}$:

$$E(A^+/{}^*A) \approx E(A^+/A) - E^{0\text{–}0} \tag{5}$$

$$E({}^*A/A^-) \approx E(A/A^-) + E^{0\text{–}0} \tag{6}$$

Detailed discussions of the kinetics aspects of electron- and energy-transfer processes can be found in the literature [11,18–20].

1.2.2 Supramolecular Photochemistry

A supramolecular system can be preorganized so as to favor the occurrence of electron- and energy-transfer processes [10]. The molecule that has to be excited, A, can indeed be placed in the supramolecular structure nearby a suitable molecule, B.

For simplicity, we consider the case of an A–L–B supramolecular system, where A is the light-absorbing molecular unit [Eq. (7)], B is the other molecular unit involved with A in the light-induced processes and L is a connecting unit (often called bridge). In such a system, after light excitation of A there is no need to wait for a diffusion-controlled encounter between *A and B as in molecular photochemistry, since the two reaction partners can already be at an interaction distance suitable for electron and energy transfer:

$$A{-}L{-}B + h\nu \rightarrow {}^*A{-}L{-}B \qquad \text{photoexcitation} \tag{7}$$

$${}^*A{-}L{-}B \rightarrow A^+{-}L{-}B^- \qquad \text{oxidative electron transfer} \tag{8}$$

$${}^*A{-}L{-}B \rightarrow A^-{-}L{-}B^+ \qquad \text{reductive electron transfer} \tag{9}$$

$${}^*A{-}L{-}B \rightarrow A{-}L{-}{}^*B \qquad \text{electronic energy transfer} \tag{10}$$

In the absence of chemical complications (e.g. fast decomposition of the oxidized and/or reduced species), photoinduced electron-transfer processes [Eqs. (8) and (9)] are followed by spontaneous back-electron-transfer reactions that regenerate the starting ground-state system [Eqs. 8′ and 9′] and photoinduced energy transfer [Eq. (10)] is followed by radiative and/or nonradiative deactivation of the excited acceptor [Eq. 10′]:

$$A^+{-}L{-}B^- \rightarrow A{-}L{-}B \qquad \text{back oxidative electron transfer} \tag{8′}$$

$$A^{-}-L-B^{+} \rightarrow A-L-B \qquad \text{back reductive electron transfer} \qquad (9')$$

$$A-L-{}^{*}B \rightarrow A-L-B \qquad \text{excited state decay} \qquad (10')$$

In supramolecular systems, electron- and energy-transfer processes are no longer limited by diffusion and occur by first-order kinetics. As a consequence, in suitably designed supramolecular systems these processes can involve even very short-lived excited states.

1.3
Wire-Type Systems

An important function at the molecular level is photoinduced energy and electron transfer over long distances and/or along predetermined directions. This function can be performed by rod-like supramolecular systems obtained by linking donor and acceptor components with a bridging ligand or a spacer.

1.3.1
Molecular Wires for Photoinduced Electron Transfer

Photoinduced electron transfer in wire-type supramolecular species has been extensively investigated [6,10]. The minimum model is a *dyad*, consisting of an electron donor (or acceptor) chromophore, an additional electron acceptor (or donor) moiety and an organizational principle that controls their distance and electronic interactions (and therefore the rates and yields of electron transfer). A great number of such dyads have been constructed and investigated [6,10].

The energy-level diagram for a dyad is schematized in Figure 1.3. All the dyad-type systems suffer to a greater or lesser extent from rapid charge recombination

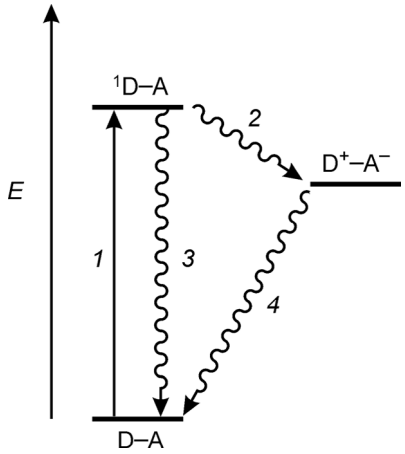

Figure 1.3 Schematic energy-level diagram for a dyad.

[process (4)]. An example of a systematic study on dyads is that performed on compounds $\mathbf{1}^{5+}$–$\mathbf{5}^{5+}$ (Figure 1.4) [21,22]. When excitation is selectively performed in the Ru(II) chromophoric unit, prompt intersystem crossing from the originally populated singlet metal-to-ligand charge-transfer (^{1}MLCT) excited state leads to the long-lived ^{3}MLCT excited state which lies ~2.1 eV above the ground state, can be oxidized approximately at −0.9 V (vs. SCE) and has a lifetime of ~1 μs in deaerated solutions [23]. Before undergoing deactivation, such an excited state transfers an electron to the Rh(III) unit, a process that is then followed by a back electron-transfer reaction.

Comparison of compounds $\mathbf{1}^{5+}$ and $\mathbf{2}^{5+}$ shows that, despite the longer metal–metal distance, the forward electron transfer is faster across the phenylene spacer ($k = 3.0 \times 10^9\ s^{-1}$) than across the two methylene groups ($k = 1.7 \times 10^8\ s^{-1}$). This result can be related to the lower energy of the LUMO of the phenylene group, which facilitates electronic coupling. In the homogeneous family of compounds $\mathbf{2}^{5+}$–$\mathbf{4}^{5+}$, the rate constant decreases exponentially with increasing metal–metal distance.

For compound $\mathbf{5}^{5+}$, which is identical with $\mathbf{4}^{5+}$ except for the presence of two solubilizing hexyl groups on the central phenylene ring, the photoinduced electron-transfer process is 10 times slower, presumably because the substituents increase the twist angle between the phenylene units, thereby reducing electronic coupling.

Photoinduced electron transfer in three–component systems (*triads*) is illustrated in Figure 1.5 [24]. The functioning principles are shown in the orbital-type energy diagrams of the lower part the figure. In both cases, excitation of a chromophoric component (step *1*) is followed by a primary photoinduced electron transfer to a primary acceptor (step *2*). This process is followed by a secondary thermal electron-transfer process (step *3*): electron transfer from a donor component to the oxidized chromophoric component (case a) or electron transfer from the primary acceptor to a secondary acceptor component (case b). The primary process competes with excited-state deactivation (step *4*), whereas the secondary process competes with primary charge recombination (step *5*). Finally, charge recombination between remote molecular components (step *6*) leads the triad back to its initial state.

For case a, the sequence of processes indicated above (*1–2–3*) is not unique. Actually, the alternative sequence *1–3–2* would also lead to the same charge-separated state. In general, these two pathways will have different driving forces for the primary and secondary steps and thus one may be kinetically favored over the other. Occasionally one of the two pathways is thermodynamically allowed and the other is not, although in a simple one-electron energy diagram like that shown in Figure 1.5a this aspect is not apparent.

The performance of a triad for wire-type applications is related to the rate and quantum yield of formation of the charge separated state (depending on the competition between forward and back processes, $\Phi = [k_2/(k_2 + k_4)][k_3/(k_3 + k_5)]$). For energy conversion purposes, important parameters are also the lifetime of charge separation (depending on the rate of the final charge-recombination process, $\tau = 1/k_6$) and the efficiency of energy conversion ($\eta_{en.conv.} = \Phi \times F$, where F is the fraction of the excited-state energy conserved in the final charge-separated state). To put things in a real perspective, it should be recalled that the "triad portion" of the

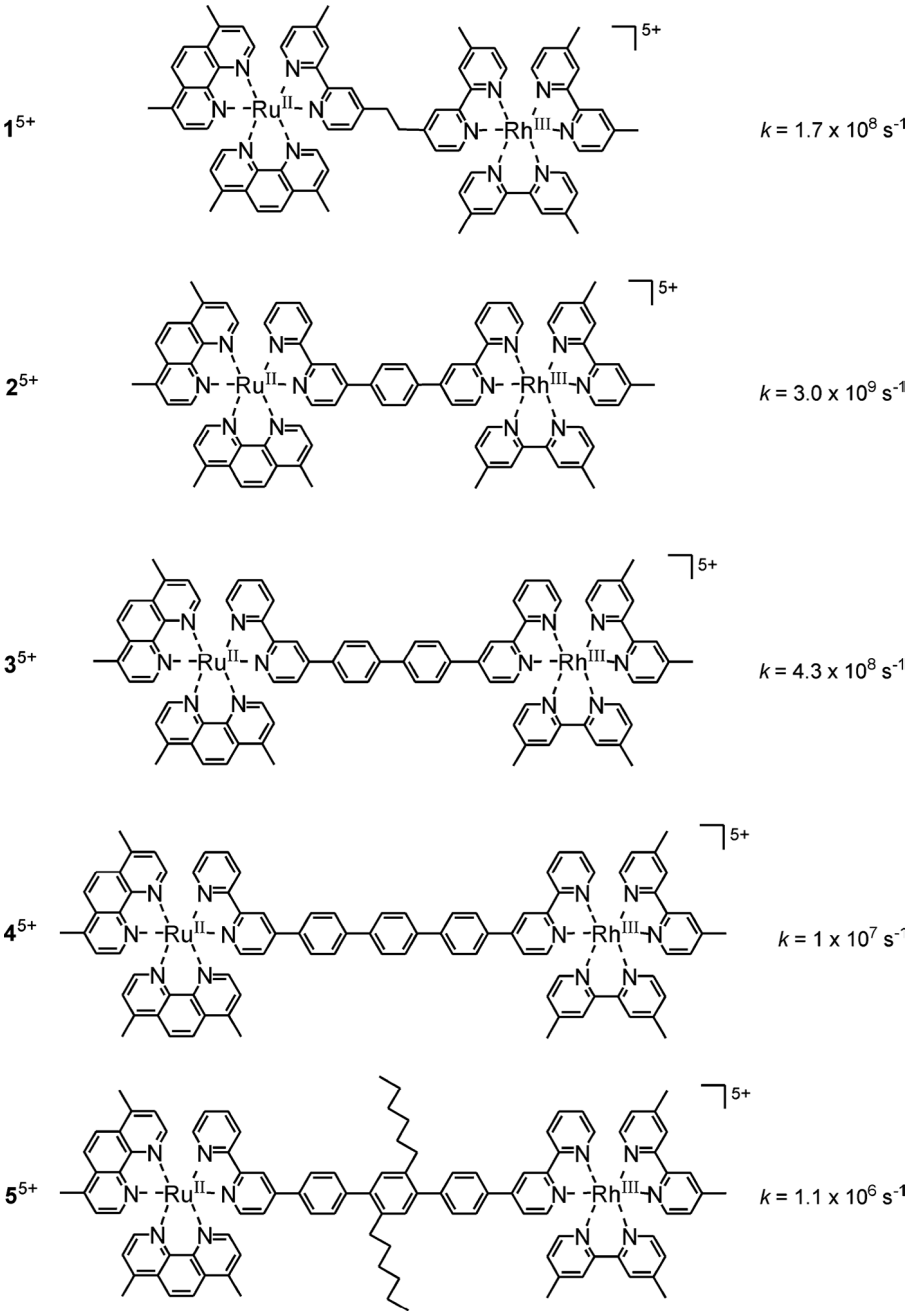

Figure 1.4 Binuclear metal complexes $\mathbf{1}^{5+}$–$\mathbf{5}^{5+}$ used for photoinduced electron-transfer experiments [21,22].

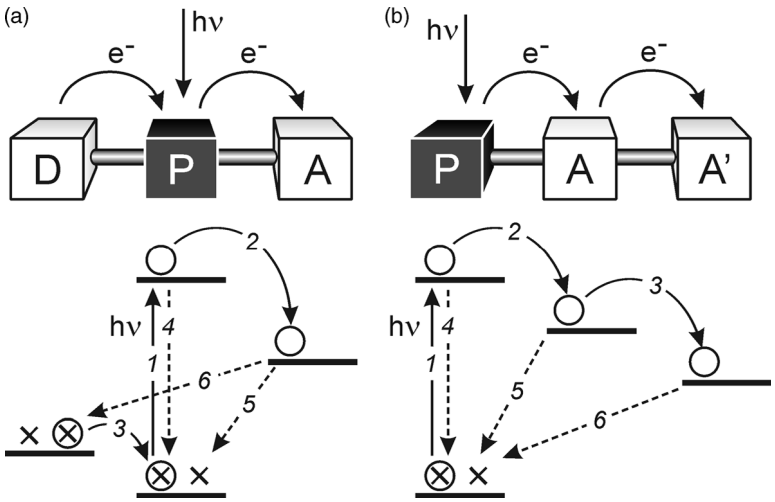

Figure 1.5 Schematic representation of the two possible arrangements for charge-separating triads.

reaction center of bacterial photosynthesis converts light energy with $\tau \approx 10\,\text{ms}$, $\Phi = 1$ and $\eta_{\text{en.conv.}} \approx 0.6$.

The introduction of further molecular components (*tetrads* and *pentads*) leads to the occurrence of further electron-transfer steps, which, in suitably designed systems, produce charge separation over larger and larger distances [6,10]. As the number of molecular components increases, also the mechanistic complexity increases and charge separation may involve energy-transfer steps.

Several triads have been designed and investigated. A very interesting system is the 4-nm long triad $\mathbf{6}^{3+}$ shown in Figure 1.6, which consists of an Ir(III) bis-terpyridine

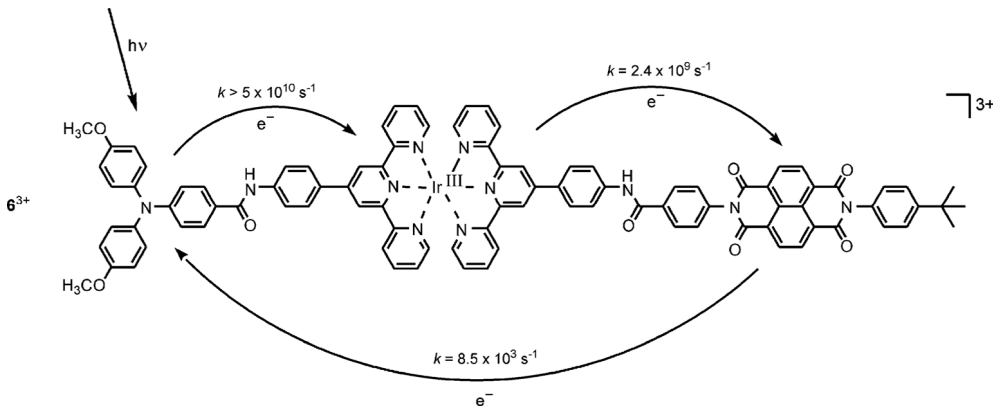

Figure 1.6 Electron-transfer processes in triad $\mathbf{6}^{3+}$ [25].

complex connected to a triphenylamine electron donor (D) and a naphthalene bisimide electron acceptor (A) [25]. Upon excitation of the electron donor D (or even the Ir-based moiety), a charge separated state D^+–Ir^-–A is formed with 100% yield in less than 20 ps that successively leads to D^+–Ir–A^- with 10% efficiency in 400 ps. Remarkably, the fully charge-separated state D^+–Ir–A^- has a lifetime of 120 μs at room temperature in deaerated acetonitrile solution.

1.3.2
Molecular Wires for Photoinduced Energy Transfer

Many investigations on electronic energy transfer in supramolecular species have been performed in the past few years [6,10], a relevant fraction of which have been obtained for systems containing polypyridine metal complexes as donor and acceptor units. Usually, the photoexcited chromophoric group is $[Ru(bpy)_3]^{2+}$ (bpy = 2,2′-bipyridine) and the energy acceptor is an $[Os(bpy)_3]^{2+}$ unit. The excited state of $[Ru(bpy)_3]^{2+}$ playing the role of energy donor is the lowest, formally triplet, metal-to-ligand charge-transfer excited state, ^{3}MLCT, which, as we have seen above, can be obtained by visible light excitation ($\lambda_{max} \approx 450$ nm), lies ~2.1 eV above the ground state and has a lifetime of ~1 μs in deaerated solutions [23]. This relatively long lifetime is very useful because it permits the study of energy transfer over long distances. The occurrence of the energy-transfer process promotes the ground-state $[Os(bpy)_3]^{2+}$ acceptor unit to its lowest energy excited state ^{3}MLCT, which lies approximately 0.35 eV below the donor excited state. Both the donor and the acceptor excited states are luminescent, so that the occurrence of energy transfer can be monitored by quenching and/or sensitization experiments with both continuous and pulsed excitation techniques.

Ru(II) and Os(II) polypyridine units have been connected by a variety of bridging ligands and spacers. When the metal-to-metal distance is very short, fast energy transfer occurs by a Förster-type resonance mechanism [26]. In other systems the two photoactive units are separated by a more or less long spacer. When the spacer is flexible [e.g. $-(CH_2)_n-$ chains], the geometry of the system is not well defined and it is difficult to rationalize the results obtained.

These problems are overcome by using rigid and modular spacers to connect the two chromophoric units; the systems so obtained have a well-characterized geometry and the energy transfer can occur over long distances. Interesting examples of this type of systems are the $[Ru(bpy)_3]^{2+}$–$(ph)_n$–$[Os(bpy)_3]^{2+}$ (ph = 1,4-phenylene; $n = 2$, 3, 4, 5) species [27] shown in Figure 1.7. In such compounds, excitation of the $[Ru(bpy)_3]^{2+}$ moiety is followed by energy transfer to the $[Os(bpy)_3]^{2+}$ unit, as shown by the sensitized emission of the latter (CH_3CN, 293 K). The energy-level diagram is shown schematically in Figure 1.7. The lowest energy level of the bridge decreases slightly as the number of phenylene units is increased, but always lies above the donor and acceptor levels involved in energy transfer. A further decrease in the energy of the triplet excited state of the spacer would be expected to switch the energy-transfer mechanism from superexchange-mediated to hopping, similar to what happens for photoinduced electron transfer. In the series of compounds shown in

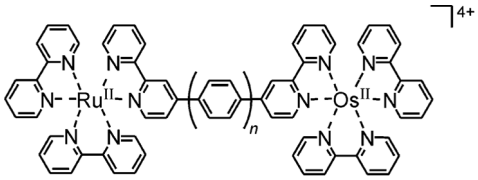

$n = 2$ $k_{en} = 2.5 \times 10^{11}\ s^{-1}$
$n = 3$ $k_{en} = 5.9 \times 10^{10}\ s^{-1}$
$n = 4$ $k_{en} = 4.1 \times 10^{9}\ s^{-1}$
$n = 5$ $k_{en} = 4.9 \times 10^{8}\ s^{-1}$

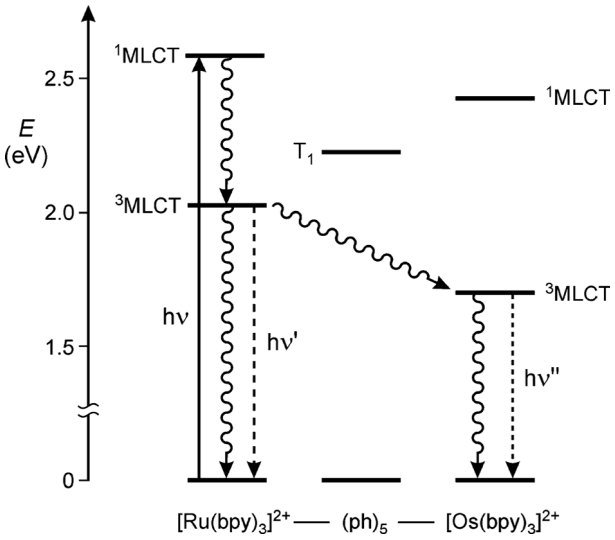

Figure 1.7 Structure of compounds $[Ru(bpy)_3]^{2+}$–$(ph)_n$–$[Os(bpy)_3]^{2+}$ and energy-level diagram for the energy-transfer process [27].

Figure 1.7, the energy-transfer rate decreases with increasing length of the oligophenylene spacer. Such rate constants are much higher than those expected for a Förster-type mechanism, whereas they can be accounted for by a superexchange Dexter mechanism [28]. The values obtained for energy transfer in the analogous series of compounds $[Ru(bpy)_3]^{2+}$–$(ph)_nR_2$–$[Os(bpy)_3]^{2+}$ [29], in which the central phenylene unit carries two hexyl chains, are much lower than those found for the unsubstituted compounds, most likely because the bulky substituents R increase the tilt angle between the phenyl units. A strong decrease in the rate constant is observed when the Ru-donor and Os-acceptor units are linked via an oligophenylene bridge connected in the meta position [30].

In an another family of similar compounds, $[Ir(ppyF_2)_2(bpy)]^{+}$–$(ph)_n$–$[Ru(bpy)_3]^{2+}$ (ph = 1,4-phenylene; $n = 2, 3, 4, 5$) [31], the energy-transfer rate constant is much higher and substantially independent of the length of the spacer. The energy-level